

## Capacitance Voltage Characteristics and Electron Holography on Cubic AlGaN/GaN Heterojunctions

Donat J. As<sup>1\*</sup>, Alexander Zado<sup>1</sup>, Qiyang Y. Wei<sup>2</sup>, Ti Li<sup>2</sup>, Jingyi Y. Huang<sup>2</sup>, and Fernando A. Ponce<sup>2</sup>

<sup>1</sup>Department Physik, Universität Paderborn, Warburger Str. 100, 33098 Paderborn, Germany

<sup>2</sup>Department of Physics, Arizona State University, Tempe, AZ 85287-1504, U.S.A.

E-mail: d.as@uni-paderborn.de

Received October 15, 2012; revised December 6, 2012; accepted December 18, 2012; published online May 20, 2013

Cubic  $\text{Al}_x\text{Ga}_{1-x}\text{N}/\text{GaN}$  heterostructures were grown by plasma-assisted molecular beam epitaxy on free-standing 3C-SiC(001). The samples consist of an unintentionally doped 600 nm thick c-GaN buffer and a 30 nm c-Al<sub>0.3</sub>Ga<sub>0.7</sub>N layer. Capacitance–voltage measurements were performed on metal–oxide–semiconductor heterojunction structure using SiO<sub>2</sub> as an insulator. A depth profile of the net donor concentration  $N_{CV}$  of the grown sample was measured, demonstrating a clear carrier accumulation at the heterojunction. By electron holography in a transmission electron microscope the potential profile was measured and a free electron concentration of  $5.1 \times 10^{11} \text{ cm}^{-2}$  was estimated at the c-Al<sub>x</sub>Ga<sub>1-x</sub>N/GaN interface. Using a one-dimensional (1D) Poisson simulator the results of both techniques are compared and a conduction-to-valence band offset ratio of about 4 : 1 for the cubic Al<sub>x</sub>Ga<sub>1-x</sub>N/GaN interface is estimated, which promotes the electron accumulation. Our results demonstrate that the two-dimensional electron gas (2DEG) in cubic Al<sub>x</sub>Ga<sub>1-x</sub>N/GaN heterostructures can be achieved without the need of polarization effects and is due to the residual background doping in the Al<sub>x</sub>Ga<sub>1-x</sub>N and GaN. © 2013 The Japan Society of Applied Physics

### 1. Introduction

Recently, the first heterojunction field effect transistor (HFET) with normally off characteristics based on non-polar cubic Al<sub>x</sub>Ga<sub>1-x</sub>N/GaN hetero-structure<sup>1)</sup> has been realized. For such devices one of the most crucial parameter that determines the physics in hetero-structures and for the optimization and design of electronic devices is the electronic band alignment at the interface between Al<sub>x</sub>Ga<sub>1-x</sub>N and GaN. Therefore, one is interested in the conduction-band offset (CBO) and the valence-band offset (VBO), which reflect how the band-gap difference of the involved semiconductor materials is portioned between the discontinuities of the occupied and unoccupied energy bands.<sup>2)</sup> In cubic nitrides grown along the (001) direction all piezoelectric polarization components should vanish and the carrier accumulation shall be due to unintentional or intentional doping of the epilayers. The absence of polarization effects is one of the advantages of cubic group III nitrides over the hexagonal group III nitrides. However, there is limited experimental understanding of the electronic band structure of cubic nitride heterostructures. In particular, accumulation of carriers at the Al<sub>x</sub>Ga<sub>1-x</sub>N/GaN interface has been observed but its origin is not well understood.

In this work we use two independent methods to determine the conduction band discontinuity and the two-dimensional electron gas (2DEG) carrier concentration, namely capacitance–voltage (C–V) measurements and electron holography in the transmission electron microscope (TEM).<sup>3)</sup> The measured results are compared with calculations of the band structure and charge carrier distribution using a one-dimensional (1D) Poisson simulator.

### 2. Experimental Procedure

A cubic Al<sub>0.3</sub>Ga<sub>0.7</sub>N/GaN heterostructure was grown by plasma-assisted molecular beam epitaxy (MBE) at 720 °C on free-standing 3C-SiC(001) substrate<sup>4,5)</sup> with GaN and Al<sub>x</sub>Ga<sub>1-x</sub>N layer thickness of 600 and 30 nm, respectively. The layer thickness was measured in-situ by reflection high-energy electron diffraction (RHEED) oscillations and ex-situ by reflectance measurements. The structural properties of

the samples were characterized by high-resolution X-ray diffraction (HRXRD) measurements.<sup>6)</sup> From a reciprocal space map (RSM) of the grown sample around the asymmetric (113) reflection we obtain the information that the 30 nm thick Al<sub>x</sub>Ga<sub>1-x</sub>N layer is pseudomorphic on the GaN buffer and that the aluminum mole fraction is 0.3, respectively.

Because of the high conductivity of the 3C-SiC substrates, the doping concentration in our samples could not be obtained by Hall-effect measurements. Therefore, C–V measurements on metal–oxide–semiconductor heterostructures (MOSH) have been performed to determine the background carrier density  $N_{CV}$  and the carrier density profile of the cubic Al<sub>x</sub>Ga<sub>1-x</sub>N/GaN hetero-structure. A SiO<sub>2</sub> layer was used as the oxide and was deposited by plasma enhanced chemical vapor deposition (PECVD) in a PECVD system from Oxford Instruments. The basic process for deposition of SiO<sub>2</sub> films in the “Plasmalab PECVD System 100” uses a mixture of 5% silane diluted in nitrogen as the silicon source, and nitrous oxide as the oxygen source. The additional PECVD process parameters were N<sub>2</sub>O flow 700 sccm, pressure 400 mTorr, RF power 5 W at 13.56 MHz and the substrate temperature was 300 °C, respectively. Using standard lithography a round contact structure with a diameter of 50 μm was placed on the top of the oxide layer. Metal gate contacts were thermally evaporated consisting of 15 nm Ni and 50 nm Au. The ohmic contact was realized by soldering the free-standing 3C-SiC on a Cu plate with In. The C–V measurements were done with an Agilent E4980A universal LCR meter. On the gate contact, a direct voltage in a range between –10 and +5 V was applied. The ohmic contact at the backside of the sample was grounded. The amplitude of the alternating voltage was 50 mV and the frequency was 2 MHz.

Cross-sectional thin samples were prepared for TEM using standard mechanical wedge polishing and argon-ion milling techniques. The electron holography measurements were performed on a Philips CM200 field-emission transmission electron microscope operating at 200 keV and equipped with an electrostatic biprism. All electron holograms were recorded using a charge-coupled device camera.

The electron holography measurements were performed to study the electrostatic potential profile of the cubic  $\text{Al}_x\text{Ga}_{1-x}\text{N}/\text{GaN}$  hetero-structure. In electron holography, the phase of the electron passing through the sample is affected by the electrostatic potential in the crystal. The phase shift in the electron beam traveling across the specimen, with respect to the electron beam in vacuum, is  $\phi(x, y) = C_E V(x, y)(t)$ , where  $C_E$  is constant for a fixed electron accelerating voltage ( $C_E = 7.28 \times 10^{-3}$  rad V $^{-1}$  nm $^{-1}$  for 200 keV electrons),  $V(x, y)$  is the projected electrostatic potential of the sample, and  $t$  is the sample thickness.<sup>7)</sup> Using the holographic method, we digitally retrieve the phase shift  $\phi(x, y)$  from the original hologram, acquire the distribution of the electrostatic potential  $V(x, y)$ , and integrate along the growth plane to obtain the 1D potential profile. More details about electron holography measurements for 2DEG and 2D hole gas (2DHG) in group III nitride heterostructures can be found elsewhere.<sup>8,9)</sup>

### 3. Results

#### 3.1 C–V measurements

The electron concentration  $N_{CV}$  at the c-Al<sub>0.3</sub>Ga<sub>0.7</sub>N/GaN interface was obtained from C–V measurements that were performed on a MOSH at 2 MHz. The inset of Fig. 1 shows the measured capacity as a function of the applied voltage for the used MOSH structure with a 22 nm thick SiO<sub>2</sub> insulator. By decreasing the gate voltage the depletion zone increases, so the C–V measurement gives a depth profile of the sample. The C–V curve contains three main parts, which are referred to the Al<sub>0.3</sub>Ga<sub>0.7</sub>N barrier layer, the 2DEG layer and the GaN layers. The range from +5.0 to 0 V belongs to the 30 nm thick Al<sub>0.3</sub>Ga<sub>0.7</sub>N layer. The form of this range depends on the donor concentration in the  $\text{Al}_x\text{Ga}_{1-x}\text{N}$  sheet and the Al content. The region of the most interest is near about 0 V. This section is referred to the 2DEG. The capacitance is almost constant or changes slightly in this voltage range. This behavior is caused by the strong localized charge carrier concentration at the heterointerface. At higher reverse biases (between –2 and –10 V) the capacity shows a square dependence on voltage, which is characteristic for a constant carrier concentration. Therefore, this range is attributed to the cubic GaN epilayer with a constant background doping.

The C–V data were used to calculate the apparent carrier density  $N_{CV}$  in the sample using the following equations:<sup>10)</sup>

$$N_{CV} = -\frac{C^2}{\epsilon\epsilon_0 A^2} \frac{dV}{dC}, \quad (1)$$

$$z_{CV} = \frac{\epsilon\epsilon_0 A}{C}, \quad (2)$$

where  $z_{CV}$  is equal to the distance from the surface and  $A$  is the contact area. The resulting carrier  $N_{CV}$  profile is depicted in Fig. 1 (red dots), where the electron density is plotted versus the distance  $z_{CV}$  from the surface. At a depth of about 30 nm a clear accumulation of electrons is seen at the Al<sub>0.3</sub>Ga<sub>0.7</sub>N/GaN heterointerface with a peak carrier concentration of about  $N_{CV} \cong 8 \times 10^{18}$  cm $^{-3}$ . By the integration of the measured  $N_{CV}$  curve an electron channel at the c-AlGaN/GaN interface with a sheet carrier density of  $n_{sh} \cong 2 \times 10^{12}$  cm $^{-2}$  is found. In a previous work we have

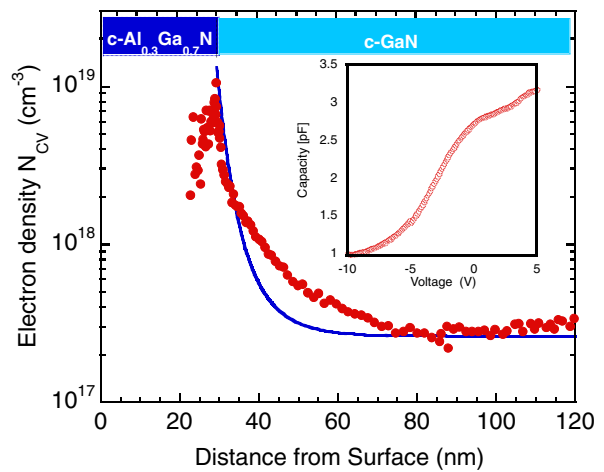


**Fig. 1.** (Color online) Measured (red dots) and calculated (blue full line) carrier density profile  $N_{CV}$  of the cubic Al<sub>0.3</sub>Ga<sub>0.7</sub>N/GaN heterostructure. The inset shows the C–V curve of the MOSH structure.

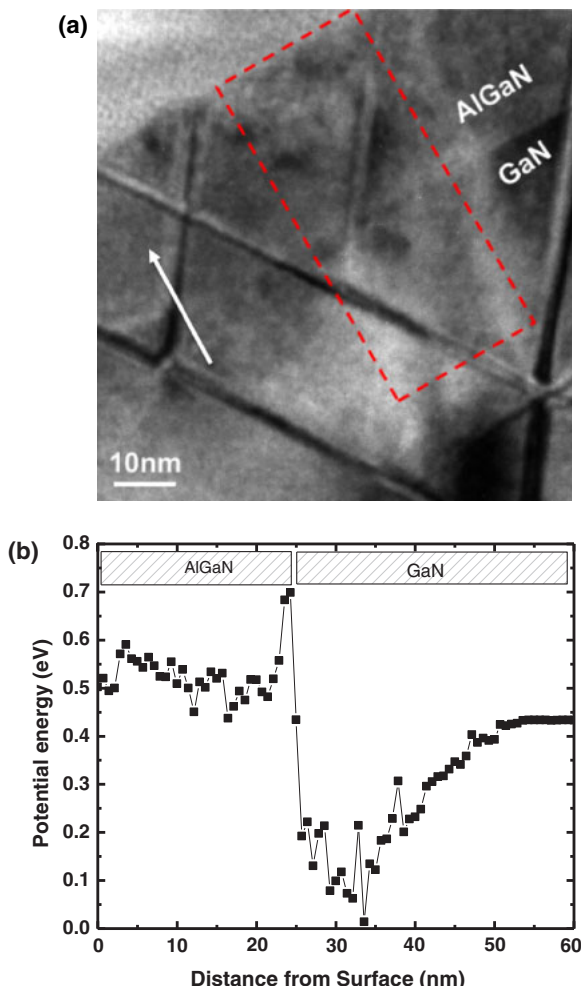
shown that this carrier accumulation results in an additional photoluminescence peak at 3.250 eV, which can be attributed to a 2DEG due to its electrical field dependence.<sup>11)</sup> The  $N_{CV}$  values measured at depths above 80 nm of  $3 \times 10^{17}$  cm $^{-3}$  and at 20 nm of  $2 \times 10^{18}$  cm $^{-3}$ , are attributed to the background carrier concentrations of cubic GaN and Al<sub>0.3</sub>Ga<sub>0.7</sub>N layers, respectively. These values are in good agreement with earlier C–V results measured on MOS structures<sup>6)</sup> and on Schottky barrier devices<sup>12)</sup> and are used in our simulations.

The blue curve in Fig. 1 shows the calculated carrier density profile using a Poisson–Schrödinger model (PSM).<sup>13)</sup> For this self-consistent calculation a donor concentration of  $3 \times 10^{17}$  and  $2 \times 10^{18}$  cm $^{-3}$  in the cubic GaN and Al<sub>0.3</sub>Ga<sub>0.7</sub>N, respectively has been assumed and a value of 0.61 eV has been used for the conduction band discontinuity  $\Delta E_c$ . This value for  $\Delta E_c$  is a reasonable value as discussed in Sect. 3.3. Good agreement between the measurement points and the simulation curve is observed without the need of polarization effects, indicating that the 2DEG is due to charge transfer from the Al<sub>0.3</sub>Ga<sub>0.7</sub>N barrier. Assuming a width of 20 nm for the two dimensional electron channel at the hetero-interface the sheet carrier concentration is calculated to  $2 \times 10^{12}$  cm $^{-2}$ .

Secondary ion mass spectroscopy measurements<sup>14)</sup> indicated that oxygen may be the reason for this background carrier concentration. In analogy to the discussion of the growth of hexagonal AlGaN with plasma-assisted MBE<sup>15)</sup> we suspect the nitrogen gas used in the plasma source as the source of oxygen, however the Al and Ga sources cannot be excluded.

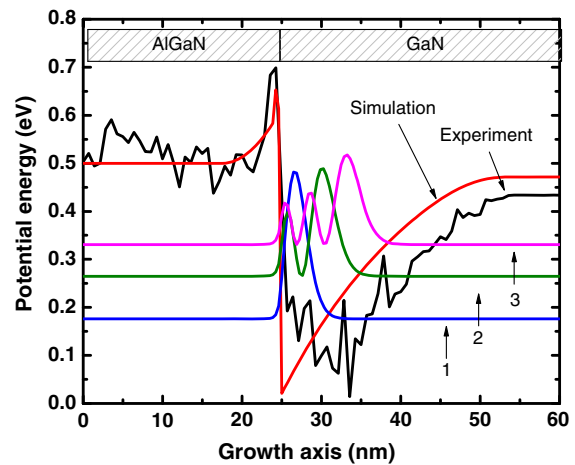
#### 3.2 Electron holography

Figure 2(a) is a cross-section TEM image of the cubic Al<sub>0.3</sub>Ga<sub>0.7</sub>N/GaN heterostructure. The crystal defects are mainly microtwins along {111} planes, which are common in cubic thin films.<sup>16,17)</sup> Electron holography was performed on the region marked by the rectangle, and the integrated thickness and phase profiles are taken (not shown here).<sup>9)</sup> The TEM specimen has a uniform thickness in the GaN region, but the AlGaN layer becomes thinner toward the



**Fig. 2.** (Color online) The cubic Al<sub>0.3</sub>Ga<sub>0.7</sub>N/GaN heterostructure in cross section: (a) TEM image along a (110) projection showing microtwins typical in cubic GaN epitaxy. The [001] direction is indicated by an arrow. (b) Potential energy profile obtained by dividing the phase and amplitude profiles from the electronic hologram.

surface. This is due to preferred oxidation and removal of the Al-containing region during ion milling. Thus, a polynomial fitting is applied to obtain the thickness profile in the AlGaN layer. The electrostatic potential profile is then obtained by dividing the phase shift by the thickness profiles; the result is shown in Fig. 2(b). In the GaN layer, the potential has a negative curvature, which indicates carrier depletion and free electrons accumulation at the GaN/AlGaN interface. The potential becomes flat in GaN at  $\sim 20$  nm away from the interface, suggesting the free electrons are confined within that range, hence have a quasi-two-dimensional characteristic. A sheet carrier concentration  $5.1 \times 10^{11}/\text{cm}^2$  is obtained from the potential curvature using Poisson's equation; this value is about one order of magnitude smaller than the density of typical wurtzite GaN 2DEG.<sup>18)</sup> However, the obtained electrical data are in good agreement (within a factor of four) with the conventional C-V measurements on these cubic AlGaN/GaN heterostructures as shown in the chapter above. A positive curvature of the potential energy profile in the AlGaN region is also observed, indicating an ionized donor density which is not negligible. This supports the idea that due to the absence of spontaneous polarization in cubic group III



**Fig. 3.** (Color online) Simulated conduction band profile compared with the electrostatic potential obtained by electron holography.

nitrides the 2DEG originates from the donor states in the AlGaN layer similar as in the case of AlGaAs/GaAs heterojunctions. At the AlGaN/GaN interface a potential drop of about  $\sim 0.65$  eV is estimated, which represents the conduction band discontinuity for the cubic Al<sub>0.3</sub>Ga<sub>0.7</sub>N/GaN heterostructure. The electron holography measurement of the potential profile has an overall error of 15% in this experiment, mainly from the estimation of thickness and from residual diffraction contrast effects.

### 3.3 Conduction band discontinuity

To better understand this quasi 2DEG in cubic AlGaN/GaN, more information about the band-edge of cubic nitrides is needed. The potential energy determined by electron holography can be understood as the conduction band for our case since the unintentionally doped nitride is typically n-type, and holography measurements provide a profile of the electrostatic potential experienced by the electrons in the conduction band. Hence, our experimental results suggest a conduction-to-valence band offset ratio at least as large as 4 : 1 for cubic AlGaN/GaN. With our measured energy band values, the electronic band diagram can again be calculated by solving the Poisson and Schrodinger equations self-consistently, where charge neutrality from donors and free electrons are satisfied. The simulated potential energy profile compared with the experimental data is shown in Fig. 3. In the simulation, an effective n-doping level of  $2 \times 10^{18} \text{ cm}^{-3}$  in the AlGaN depletion region is used, and a zero polarization field for cubic nitride is assumed. The first three electron states are also shown in the figure, which indicates the carriers' distribution is limited in a characteristic length less than 20 nm, in a quasi-2D nature. The potential drop of about  $\sim 0.65$  eV represents the conduction band discontinuity at the cubic Al<sub>0.3</sub>Ga<sub>0.7</sub>N/GaN heterostructure.

Recently, inter-sub-band and interband spectroscopies as well as ab initio calculations predicted a conduction-to-valence band offset ratio value of 3 : 1 for cubic AlN/GaN superlattices (SL) and a valence band offset of 0.5 eV.<sup>19)</sup> For cubic AlN/GaN superlattices, however, the minimum conduction band is the X-band and not the  $\Gamma$ -Band, which dominates the optical properties of the SL structure. Room

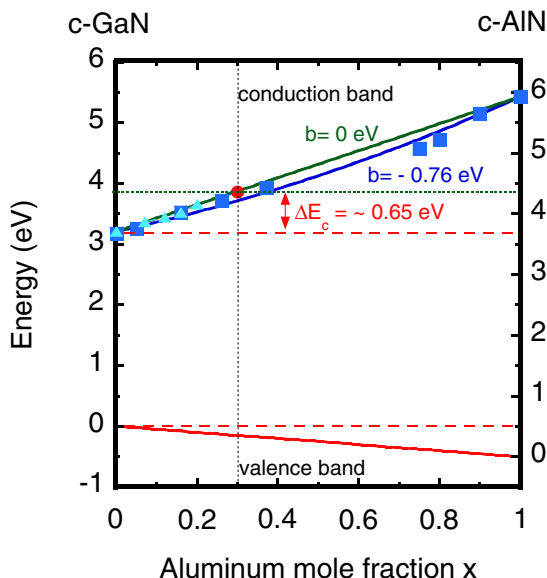


**Fig. 4.** (Color online) Band edge energies of cubic  $\text{Al}_x\text{Ga}_{1-x}\text{N}$  as a function of the compositional parameter  $x$ .

temperature ellipsometry showed that zinc-blende AlN is indeed an indirect semiconductor with an indirect gap of 5.3 eV and a direct gap of 5.93 eV.<sup>20</sup> Figure 4 depicts the band edge energy of cubic  $\text{Al}_x\text{Ga}_{1-x}\text{N}$  as a function of the compositional parameter  $x$ . In this diagram a linear dependence of the valence band with Al content and a type I band gap arrangement is supposed (full red curve). The dependence of the band gap on the Al content  $x$  can be described by the well known formula:<sup>21</sup>

$$E_g(x) = E_g(0) + [E_g(1) - E_g(0)] \cdot x + b \cdot x \cdot (1 - x), \quad (3)$$

where  $E_g(0)$  is the band gap of cubic GaN,  $E_g(1)$  the direct band gap of c-AlN and  $b$  the bowing parameter, which describes the nonlinear dependence of the band gap. For two different bowing parameters  $b = 0$  and  $-0.76$  eV the course of the conduction band is plotted in Fig. 4. Experimental data on the direct band gap of cubic of  $\text{Al}_x\text{Ga}_{1-x}\text{N}$  epilayers determined by ellipsometric measurements are also included in Fig. 4 and are all between the two curves with the different bowing parameters (blue squares<sup>22</sup> and blue triangles<sup>23</sup>). In this plot the difference between the course of the conduction band and the straight horizontal dashed red upper line represents the conduction band discontinuity  $\Delta E_c$ . For an  $\text{Al}_{0.3}\text{Ga}_{0.7}\text{N}/\text{GaN}$  heterojunction with an Al-content of  $x = 0.3$  a value between 0.69 and 0.5 eV is expected. Electron holography measured a conduction band discontinuity  $\Delta E_c = 0.65$  eV. This value is drawn in Fig. 4 by the full red circle and fits excellently with our consideration. The consistency of experimental and theoretical data demonstrates that the free electron accumulation is induced by the donor states in the  $\text{Al}_{0.3}\text{Ga}_{0.7}\text{N}$  layer, and promoted by the large conduction band-offset of the cubic  $\text{Al}_{0.3}\text{Ga}_{0.7}\text{N}/\text{GaN}$ .

#### 4. Conclusions

Capacitance voltage measurements and electron holography in the transmission electron microscope (TEM) are used to determine the conduction band discontinuity and the two-

dimensional electron gas carrier concentration in cubic  $\text{Al}_x\text{Ga}_{1-x}\text{N}/\text{GaN}$  hetero-structures grown by plasma-assisted molecular beam epitaxy on free standing 3C-SiC(001) substrates. A depth profile of the net donor concentration  $N_{CV}$  of the grown sample was measured, demonstrating a clear carrier accumulation at the heterojunction. By electron holography TEM the potential profile was determined and a free electron concentration of  $5.1 \times 10^{11} \text{ cm}^{-3}$  was estimated at the  $\text{c-Al}_x\text{Ga}_{1-x}\text{N}/\text{GaN}$  interface. Using a 1D Poisson simulator the results of both techniques are compared and a conduction-to-valence band offset ratio of about 4 : 1 for the cubic  $\text{Al}_x\text{Ga}_{1-x}\text{N}/\text{GaN}$  interface is estimated, which promotes the electron accumulation. Our results demonstrate that the two-dimensional electron gas in cubic  $\text{Al}_x\text{Ga}_{1-x}\text{N}/\text{GaN}$  heterostructures can be achieved without the need of polarization effects and is due to the residual background doping in the  $\text{Al}_x\text{Ga}_{1-x}\text{N}$  and GaN.

#### Acknowledgements

D. J. As acknowledges financial support from the “Deutsche Forschungsgemeinschaft” (project No. As 107/4-1) and expresses gratitude to H. Nagasawa, HOYA Corporation, SiC Development Center, Japan, who supplied the 3C-SiC substrates.

- 1) E. Tschumak and R. Granzer, J. K. N. Lindner, F. Schwierz, K. Lischka, H. Nagasawa, M. Abe, and D. J. As: *Appl. Phys. Lett.* **96** (2010) 253501.
- 2) C. Mietze, M. Landmann, E. Rauls, H. Machhadani, S. Sakr, M. Tchernycheva, F. H. Julien, W. G. Schmidt, K. Lischka, and D. J. As: *Phys. Rev. B* **83** (2011) 195301.
- 3) F. A. Ponce: *Ann. Phys. (Berlin)* **523** (2011) 75.
- 4) D. J. As: *Microelectron. J.* **40** (2009) 204.
- 5) J. Schörmann, S. Potthast, D. J. As, and K. Lischka: *Appl. Phys. Lett.* **89** (2006) 131910.
- 6) A. Zado, E. Tschumak, K. Lischka, and D. J. As: *Phys. Status Solidi C* **7** (2010) 52.
- 7) J. Cai and F. A. Ponce: *J. Appl. Phys.* **91** (2002) 9856.
- 8) Z. H. Wu, M. Stevens, F. A. Ponce, W. Lee, J. H. Ryou, D. Yoo, and R. D. Dupuis: *Appl. Phys. Lett.* **90** (2007) 032101.
- 9) Q. Y. Wei, Z. H. Wu, K. W. Sun, F. A. Ponce, J. Hertkorn, and F. Scholz: *Appl. Phys. Express* **2** (2009) 121001.
- 10) W. C. Johnson and P. T. Panousis: *IEEE Trans. Electron Devices* **18** (1971) 965.
- 11) S. Potthast, J. Schörmann, J. Fernandez, D. J. As, K. Lischka, H. Nagasawa, and M. Abe: *Phys. Status Solidi C* **6** (2006) 2006.
- 12) D. J. As, S. Potthast, J. Fernandez, J. Schörmann, K. Lischka, H. Nagasawa, and M. Abe: *Appl. Phys. Lett.* **88** (2006) 152112.
- 13) I. H. Tan, G. Snider, and E. L. Hu: *J. Appl. Phys.* **68** (1990) 4071.
- 14) A. Zado, J. Gerlach, and D. J. As: *Semicond. Sci. Technol.* **27** (2012) 035020.
- 15) C. R. Elsass, T. Mates, B. Heying, C. Poblenz, P. Fini, P. M. Petroff, S. P. DenBaars, and J. S. Speck: *Appl. Phys. Lett.* **77** (2000) 3167.
- 16) F. A. Ponce and J. Aranovich: *Appl. Phys. Lett.* **38** (1981) 439.
- 17) F. A. Ponce, W. Stutius, and J. G. Werthen: *Thin Solid Films* **104** (1983) 133.
- 18) Z. H. Wu, M. Stevens, F. A. Ponce, W. Lee, J. H. Ryou, D. Yoo, and R. D. Dupuis: *Appl. Phys. Lett.* **90** (2007) 032101.
- 19) C. Mietze, M. Landmann, E. Rauls, H. Machhadani, S. Sakr, M. Tchernycheva, F. H. Julien, W. G. Schmidt, K. Lischka, and D. J. As: *Phys. Rev. B* **83** (2011) 195301.
- 20) M. Röppischer, R. Goldhahn, G. Rossbach, P. Schley, C. Cobet, N. Esser, T. Schupp, K. Lischka, and D. J. As: *J. Appl. Phys.* **106** (2009) 076104.
- 21) F. Sökeland, M. Rohlffing, P. Krüger, and J. Pollmann: *Phys. Rev. B* **68** (2003) 075203.
- 22) M. Röppischer: Dr. Thesis, Fakultät für Mathematik und Naturwissenschaften, TU Berlin, Berlin (2011) [in German].
- 23) A. Kasic, M. Schubert, T. Frey, U. Köhler, D. J. As, and C. M. Herzinger: *Phys. Rev. B* **65** (2002) 184302.